Tutorial: fluorescence lifetime microscopy of membrane mechanosensitive Flipper probes

Chloé Roffay, Juan Manuel García-Arcos, Pierrik Chapuis, Javier López-Andarias, Falk Schneider, Adai Colom, Caterina Tomba, Ilaria Di Meglio, Katia Barrett, Valentin Dunsing, et al.

EDITORIAL SUMMARY

A Tutorial review on the measurement of membrane mechanical forces reported via fluorescence lifetime variations induced by conformational changes of the Flipper probes.

Tutorial: fluorescence lifetime microscopy of membrane mechanosensitive Flipper probes

Chloé Roffay[1], Juan Manuel García-Arcos[1], Pierrik Chapuis[1], Javier López-Andarias[2,3], Falk Schneider[4], Adai Colom[5,6,7], Caterina Tomba[8], Ilaria Di Meglio[1], Katia Barrett[9], Valentin Dunsing[9], Stefan Matile[2,3], Aurélien Roux[1,3]*, Vincent Mercier[1,3]*

[1]Department of Biochemistry, University of Geneva, CH-1211 Geneva, Switzerland.
[2]Department of Organic Chemistry, University of Geneva, CH-1211 Geneva, Switzerland
[3]National Center of Competence in Research in Chemical Biology, University of Geneva, CH-1211 Geneva, Switzerland.
[4] Translational Imaging Center, University of Southern California, Los Angeles, CA 90089, United States of America
[5] Biofisika Institute (CSIC, UPV/EHU), ES-48940 Leioa, Spain;
[6] Department of Biochemistry and Molecular Biology, Faculty of Science and Technology, Campus Universitario, University of the Basque Country (UPV/EHU), ES-48940 Leioa, Spain
[7] IKERBASQUE, Basque Foundation for Science, 48013 Bilbao, Spain
[8] CNRS, INSA Lyon, Ecole Centrale de Lyon, Universite Claude Bernard Lyon 1, CPE Lyon, INL, UMR5270, 69621 Villeurbanne, France
[9] Aix-Marseille Université & CNRS, IBDM - UMR7288 & Turing Centre for Living Systems, Parc Scientifique de Luminy FR-13288 Marseille, France

*Correspondence to: aurelien.roux@unige.ch, vincent.mercier@unige.ch.

Abstract:

Measuring forces within living cells remains a technical challenge. In this Tutorial, we cover the development of hydrophobic mechanosensing fluorescent probes called Flippers, whose fluorescence lifetime depends on lipid packing. Flipper probes can therefore be used as reporters for membrane tension via the measurement of changes in their fluorescence lifetime. We describe the technical optimization of the probe for imaging and provide working examples for their characterizations in a variety of biological and in vitro systems. We further provide a guideline to measure biophysical parameters of cellular membranes by FLIM microscopy using Flipper probes, providing evidence that flippers can report long range forces in cells, tissues, and organs.

Introduction

Measuring physical forces in biological samples is technically challenging [1]. Microscopy-based approaches are often preferred because they are less invasive than other mechanical methods and the necessary equipment is available in most research facilities. Fluorescence-based tools, such as Forster Resonance Energy Transfer (FRET) biosensors, allows the measurements because the elongation of a linker between two FRET fluorophores under force

reduces the FRET efficiency, and can thus be measured. The FRET couple and the linker can be composed of fluorescent proteins connected by a peptide chain, all of which can be easily expressed in cells using standard molecular biology techniques. This approach has been used to measure forces at focal adhesions, and has been extended to measure forces between membranes and actin[2], the cytoskeleton and the nucleoskeleton [3] or membrane domains[4]. However, these biosensors have several limitations, namely that the force range detectable is very small, and thus require the use of several chimeric constructs with different linkers. Also, the force sensor needs to be bound to protein "handles" onto which the force is applied which in turn means that finding the right combination of interacting domains that will not detach under force remains challenging.

Another strategy has been to design small chemicals whose fluorescence properties change under force variation. For example, molecular rotors report change in membranes viscosity by variations of their fluorescence lifetime, measured by Fluorescence Lifetime Imaging Microscopy (FLIM) [5,6]. The main limitation of molecular rotors is the limited spectrum of forces that can be measured and the fact that viscosity strongly depends on several environmental parameters.

Flipper probes are small molecules which can report changes of membrane lateral forces (due to lipid packing variations) through changes of their conformation and hence of their fluorescent properties[7]. Flippers can report membrane tension variations via a large range of lifetime values [8], for example upon osmotic shocks [9–11]. Flipper probes have already been extensively used to investigate the role of lipid packing [12–14] as well as cellular processes such as: cytoskeleton remodelling [10,15], exocytosis [16,17], TORC2 pathway [18,19], adipogenesis [20], nuclear membrane properties [21], membrane properties at nucleation zone [22], 3D cellular migration [23] or crypt morphogenesis [24].

Over the past six years, we designed various derivatives targeting different organelles[25] (plasma membrane, endoplasmic reticulum, mitochondria and lysosome/late endosome), which are commercially available at spirochrome.ch, or local providers. We also developed probes with different biochemical and/or photochemical properties[6] (HaloFlipper, HaloPhotoFlipper, HydroFlipper). We identified fluorescence lifetime imaging (FLIM) as the best way to report the conformational changes of Flipper probes with lipid packing because the amplitude of lifetime variation is higher than the change of fluorescence intensity or wavelength shift.

However, measuring membrane tension using FLIM of Flippers remains technically challenging. This method paper provides technical and practical information to make the use of Flipper probes for membrane tension measurements more accessible and reproducible.

Flipper probe basics

There are currently four commercialized Flipper probes with identical mechano-chemistry principles, targeting different membranes in cells: Flipper-TR for plasma membrane, ER Flipper-TR for endoplasmic reticulum, Lyso Flipper-TR[25] for late endo/lysosomes and Mito Flipper-TR for mitochondria. The common chemical structure of Flipper probes (see Fig 1a) is composed of two dithienothiophenes (DTT) fluorescent groups that can rotate around the carbon bond that links them together. Methyl groups have been specifically added to ensure that the two DTT groups are twisted out of co-planarity in the ground state but can still be planarized under application of orthogonal forces. Thus, Flippers have been designed as molecular sensors for compressive forces.

As the Flipper structure is mostly hydrophobic, the molecule spontaneously inserts in between hydrophobic tails of lipids that constitute cellular membranes (Fig 1b). When inserted, the hydrophobic forces that pack the lipids into a bilayer exert pressure onto the Flipper

fluorophore and planarize it. Its planarization depends on the lipid composition, and in short, more ordered membranes exert more force and provide more planarization of Flippers and reversely, disordered membrane, less force and planarization.

The conformation (i.e. how much the Flipper molecule is planarized versus twisted) of the Flipper affects several parameters of the photo-physics of the molecule: in the planarized state, the photon emission efficiency is increased by 10x compared to the most twisted state, and the peak of photon absorption is shifted towards larger wavelength, while the change is minimal for the emission peak [26].

In particular, we noted that the lifetime of Flipper dramatically varied with lipid composition. The lifetime (τ_l or the longest decay of a bi-exponential fit) in the twisted state, equivalent to highly disordered lipid membranes, was as small as 2.3 ns, while it could reach values as high as 7 ns in highly ordered membranes, where the molecule is fully planarized. This large range of lifetime values is due to the fact that in the planarized state, fluorescence of the two fluorophores is coupled through an electron transfer from the donor group to the acceptor group[6], which delays emission of the photons, giving longer lifetimes.

The range of lifetime values that this probe can cover is larger compared to other probes. Indeed, Flippers are so sensitive that they can report tiny changes of the hydrophobic pressure linked to changes of membrane tension. In single phase membranes, increases in tension reduce the pressure exerted by lipid packing on the probe, allowing it to relax to a more twisted state, reducing its lifetime. In cell membranes or in giant unilamellar vesicles (GUVs) with phase separating lipid composition, increasing tension results in higher lifetime and decreasing tension results in a shorter lifetime. This is likely due to a tension-dependent lipid phase separation [27–29] (Fig 1c). The response of Flippers in cell membranes has been confirmed in many studies[6,8–10,18,30] and validated by molecular simulation[31]. Flippers are thus complementary to Laurdan, an organic fluorescent dye which allows to detect changes in plasma membrane fluidity by measuring its fluorescence anisotropy or its lifetime [32,33]. Flipper-TR was also compared in depth to membrane order probes[34]. Because Flippers depend on both the lipid composition and membrane tension, changes of their lifetime can be directly associated with a change in tension only in cases where lipid composition is not changing, a condition always met *in vitro*. In live cells however, we typically consider that any variation of lifetime on the second timescale is related to membrane tension, because lipid composition is unlikely to change over this timescale. For longer timescales (minutes and hours), appropriate controls are required to test whether the lipid composition is dramatically changing.

Staining biological samples with Flipper probes

In its micellar form, the hydrophobic probe in aqueous solution does not fluoresce. When the Flipper probe diffuses within lipid membranes, it inserts vertically between lipids and fluoresces. Thus, Flipper probes are "fluorogenic", becoming fluorescent only when inserted in the structure they target. We describe staining procedures, problems, and possible solutions below.

Staining of cultured cells

To label most of the cell lines tested (Fig 2a), the probe, solubilized in DiMethylSulfOxide (DMSO), was normally directly added to the imaging medium at 1 µM final concentration and incubated 15 min at 37°C with cells. For the epithelial cell line MDCK-II, the medium was replaced 1 h before imaging with medium containing 1 µM of Flipper-TR in order to allow the probe to penetrate through the cell monolayer. To keep a low concentration of DMSO in the final medium, 1 mM stock solutions of Flipper probes were usually made. In some cell types (for example HeLa Kyoto and HeLa MZ), 5 min of Flipper incubation at 37°C was enough to obtain good staining. However, at high cell density or in 3D cell cultures and tissues, longer

incubation - in the order of a few hours - was necessary to allow the probe to diffuse deep into the sample. The imaging media used for diluting the Flipper probe were Fluorobrite with HEPES or CO_2 supply, or Leibovitz if no CO_2 supply was available. The use of Foetal Bovine Serum (FBS) during staining and imaging can cause a lower signal, as it contains proteins which can extract hydrophobic molecules from membranes such as albumin. However, we haven't observed a dramatic change of labelling efficiency using solutions described above supplemented with FBS. If the staining appears to be low with FBS, we nevertheless recommend testing solutions without it. We did not observe drastic differences on the fluorescence intensity and lifetime of the probe between cells imaged at 37°C and the ones imaged at room temperature. Similarly, CO_2 adjunction in the imaging chamber or working with a medium supplemented with HEPES does not significantly impact Flipper fluorescence intensity or lifetime.

Importantly, the cell labelling occurs through a dynamic equilibrium of the probe with the micellar pool in the cell culture medium. Thus, a constant exchange of Flipper-TR between the plasma membrane and the medium occurs. This exchange is rapid for the Flipper-TR because the medium is directly in contact with the plasma membrane labelled by the probe. We thus recommend, if possible, to keep a constant Flipper-TR concentration along the experiment. Due to the dynamic exchange of the probe between the membrane and the medium, washing Flipper-TR labelled cells with medium containing no Flipper will decrease Flipper-TR staining, and even faster with FBS or BSA in the washing buffer. Therefore, if washing is absolutely needed, it is recommended to wash with medium without FBS, and/or keeping the concentration of the Flipper constant in the washes, which will limit the decrease of the plasma membrane staining.
Reaching the dynamic equilibrium takes about 5-10 minutes, thus the photon count depends on the time of incubation of cells with the probe, until it reaches a plateau value that depends on your system. Incubations that are too long may lead to Flipper-TR endocytosis and endosomal labelling. The Flipper-TR lifetimes within endosomal compartments are notably lower than in the plasma membrane (Fig 2a-c), and we have never observed Flipper-TR labelling expanding further away than from the endosomes (probably even the early endosomes). Also, the Flipper-TR endosomal labelling appeared with various times depending on the cell types and experimental conditions. In MDCK, we observed that endosomal labelling occurred after 12 hours (Fig 2d).
For long-term plasma membrane imaging experiments (several hours) with sufficient time-lapse between images, we recommend performing sample-labelling for each time point: the sample is incubated with Flipper-TR, imaged, and then the probe is washed away using medium with BSA or FBS. Each timepoint requires re-incubation of the probe to prevent Flipper-TR endocytosis.

Concerning Lyso-Flipper-TR, and most probably other organelle specific probes that were not tested in depth, the molecule diffuses freely across the plasma membrane and quickly concentrates in the membrane of late endosomes and lysosomes (in a few minutes) because the protonation of its headgroup in this acidic environment blocks its diffusion through the membrane. Consequently, for short timescale experiments (less than 2h), it is not an issue to leave cells in medium containing Lyso-Flipper-TR. However, loss of the acidity of endosomal compartments after treatments or change in the pH of the medium (due for example to phototoxicity) may trigger loss of the Lyso-Flipper-TR staining. The best labelling was obtained by incubating Lyso-Flipper-TR at 1 µM in Fluorobrite medium without serum for 20 minutes at 37°C prior to imaging.

Co-staining with Flipper-TR

To specifically analyse the tension or lipid composition of a given organelle or during a biological process, it is possible to use other fluorescent probes or stable cell lines in conjunction with Flipper probes. However, to avoid any fluorescence overlap with the probe, which could affect lifetime measurements, blue or far-red fluorescent probes should be used (e.g: Organic dyes like Alexa-405 or Alexa-647 or Blue fluorescent protein, E2-Crimson or smURFP for fusion proteins, see Fig 2e).

Flipper-TR has broad absorption and emission spectra because of its two fluorescent groups: significant absorption occurs between 420 nm and 530 nm with a peak at 485 nm, while significant emission occurs between 550 nm and 670 nm with a peak at 600 nm. Flipper fluorescence emission is thus optimally collected using a band pass 600/50 emission filter. Therefore, the configuration needed to image Flippers on a confocal is not common and needs to be personalized. For example, in the case of an organelle labelled with Alexa-405, excitation of this fluorophore (peak at 400 nm) will only weakly excite Flipper probes, limiting the phototoxicity while the emission of Alexa-405 (400-530 nm) will not go through the FLIM detector and will not interfere with Flippers lifetime measurement.

[Box 1]

Cells and organisms stained and imaged using Flipper probes

List of cell types used with Flipper-TR: HeLa MZ, HeLa Kyoto, MDCK, keratinocyte PW21, keratinocyte KRAS, mouse hippocampal primary neurons, MDA MB 231 cells (MD Anderson-Metastatic Breast-231 Cells, human breast adenocarcinoma), A549 (human lung cancer: epithelia, carcinoma), H596 (epithelial-like cell line isolated from the lung of a 73-year-old, white, male with lung Adenosquamous Carcinoma), RPE-1 (Retinal Pigment Epithelial-1), MEF (Mouse Embryonic Fibroblast) with lifetime value (τ_1) ranging from 5 ns to 5.7 ns (Fig 2a).

List of cell types used with EndoFlipper-TR: HPDE (Human Pancreatic Duct Epithelial Cell Line), KP4 (human pancreatic ductal cell carcinoma cell line derived from human ascites), Hela MZ, A431(human epidermoid carcinoma), 293T (human kidney epithelial cell), MDA MB 231 cells (MD Anderson-Metastatic Breast-231 Cells, human breast adenocarcinoma) with lifetime value (τ_1) ranging from 4.4 ns to 5.1 ns (Fig 2b).

List of cell types used with LysoFlipper-TR[6,35]: HeLa MZ, MDA with lifetime value (τ_1) ranging from 4.1 ns to 4.7 ns (Fig 2c).

List of organisms stained with Flipper-TR: alginate capsules containing cells (Figure Box-1a), alginate tubes with attached cells on the inner surface (Figure Box-1b), PDMS roll with attached cells on the inner surface (Figure Box-1c), Arabidopsis *thaliana* embryo, root and leaf (Figure Box-1d, e), Xenopus explant (Figure Box-1f), 3D gastruloids of mouse Embryonic Stem Cells (Figure Box-1g), mouse embryos (Figure Box-1h and ref [36]) or *Bacillus Subtilis* (Figure Box-1i).

List of organisms where Flipper-TR staining did not work: E. coli (Gram-negative bacteria) (Figure Box-1i, top panel). Indeed, Gram-negative E. coli showed only minimal Flipper-TR staining when compared to the Gram-positive Bacillus subtilis (Figure Box-1j), suggesting that the presence of an additional lipoprotein layer in the cell wall in of Gram-negative bacteria could prevent efficient Flipper-TR staining. Importantly, the staining in E. coli appears cytosolic while in B. subtilis Flipper-TR signal peaks at the cell boundaries (Fig Figure Box-1i), suggesting that Flipper-TR is specific to membranes only in Gram-positive bacteria. Unsuccessful Flipper staining were reported to us by other research groups: several attempts of zebrafish staining with Flipper failed so far. Drosophila S2 cells, as well as dendritic cells seem to marginally retains the flipper probes, maybe because of their high endosomal recycling rates.

Derivative probes for staining alternative targets

Various derivatives of Flipper were developed to target the endoplasmic reticulum (ER Flipper-TR), the mitochondria (Mito Flipper-TR), the lysosome/late endosome (Lyso Flipper-TR)[25] and more recently the early endosome (Endo Flipper-TR)[35] as well as a version of the probe for single-molecule super-resolution imaging of membrane tension (SR-Flipper[30,37]). The structures can be found in[6]. The ER Flipper-TR selectively labels the membranes of endoplasmic reticulum via a pentafluorophenyl group which reacts with cysteine of proteins present on ER outer surface[6,25]. The average lifetime of ER Flipper-TR is lower (3.5 ns in HeLa cells) than Flipper-TR (4.5 ns in HeLa cells) in various cell lines. The Mito Flipper-TR (Spirochrome)[6,25]; selectively labels the inner membranes of mitochondria via the interaction between the hydrophobic triphenylphosphonium cation with the negatively charged surface resulting from the negative potential of the mitochondrial inner membrane. As observed for ER Flipper-TR, the average lifetime of Mito Flipper-TR is rather low (around 3.2 ns in HeLa cells).

Lyso Flipper-TR and Endo Flipper TR contain a morpholine headgroup of higher pKa in Endo Flipper-TR compared to Lyso Flipper-TR. This morpholine group is protonated in the acidic environment of endosomes, blocking its diffusion through membranes and retaining the probe in the endosome. The average lifetime of Lyso Flipper-TR is around 4 ns in HeLa cells. Both Endo and Lyso Flipper-TR are showing very weak phototoxicity.

SR-Flipper[37] targets the plasma membrane of cells and reversibly switches from bright-state ketones to dark-state hydrates, hemiacetals, and hemithioacetals both in twisted and planarized state. It is therefore possible to use it for single-molecule localization microscopy and to resolve membranes well below the diffraction limit. The lifetime (τ_1) of SR-Flipper is usually slightly lower (~10%) than the lifetime of Flipper-TR. HaloFlipper is based on the combination of the Flipper and a Halo tag to label any membrane of interest by targeting membrane specific protein labelled with a halo tag. Halo PhotoFlipper targets the nuclear membrane and the inner plasma membrane using a photocleavable domain[38].

Fluorescence lifetime acquisition

Flipper probes have long average fluorescence lifetimes, up to 7 ns depending on membrane composition, which means that photons with lifetimes up to 50 ns have to be detected to accurately measure the lifetime. Consequently, FLIM systems with sampling frequencies of 20 MHz are the only devices to detect all the photons, allowing for most accurate Time Correlated Single Photon Counting (TCSPC) fits. We found however that the dye can also be efficiently excited using a two-photon mechanism (excitation around 880 nm 950 nm, Extended Data Figure 1a, b). Unfortunately, most two-photon microscope set-ups are only equipped with a fixed repetition rate laser pulsing at 80 MHz. Increasing the pulse rate leads to artificially shortened lifetimes in GUVs (excited with one-photon at 488 nm) (FigS1c, d, e). While the lifetime of Flipper-TR in GUVs still depends on the membrane compositions, the dynamic range is reduced at 80 MHz compare to 20 MHz (Extended Data Figure 11c, d, e). The use of Flipper-TR in conjunction with the possibility of two-photon excitation is a promising feature for in vivo studies and deep tissue imaging of tension. On PicoQuant systems the pulsed laser frequency can be set between 80 MHz and 31.25 kHz, but on LEICA systems the laser frequency is by default 80 MHz which will not allow to detect photons with lifetimes higher than 12.5 ns. This represents a substantial number of photons not being detected for a fluorophore with an average lifetime of 4 ns for instance. Therefore, the sampling frequency has to be reduced in LEICA systems, using the pulse-picker device (illuminates one out of 2 or more laser pulses), otherwise the lifetime will be underestimated. Because of the bi-exponential nature of the Flipper decay curve, it is important to detect enough photons without saturating

the detector. We recommend recording a minimum intensity peak of 10^4 photons per field of view and with at least 200 photons for the brightest pixel.
Because of the repeated sample illumination during FLIM, and the high fluorescence of Flipper probes, imaging Flippers is fairly phototoxic to cells. Several aspects have to be considered to reduce phototoxicity when imaging Flippers. First, the phototoxicity is reduced by lowering the laser pulse frequency. With classical TCSPC it is very important to have a count rate not exceeding 1 to 5% of the excitation rate (for 20MHz pulse, average detector count rate should not exceed 1 MHz) in order to maintain a low probability of detecting more than one photon per excitation cycle (because of the dead time of the detector, the system would detect the first photon and miss the second one, this is called the "pile up" effect). Other classic confocal microscopy parameters that participate in light acquisition (pinhole aperture, laser power, pixel binning, scanning speed, size of the ROI, line/frame summation) may be used to optimize photon collection.
Several approaches can be used to reduce the phototoxicity:
- Using a new generation of TCSPC device with reduced dead time (rapidFLIM from Picoquant, dead time of less than 650 ps compared to 80 ns in normal FLIM) that allows to detect more photons per excitation cycle. It also provides a better temporal resolution (see below) and allows to work with higher intensities. Overall, with this new kind of TCSPC much higher detector count rates can be processed which result in a faster acquisition. This system also allows to acquire more than one photon per laser pulse without the pile up effect.
- Repeating acquisition and summing-up photons from several images will allow to obtain sufficient counts of photons (minimum peak of 10^4 events) for a reliable fit. For standard cells in culture, we used the following conditions. For example, using Flipper-TR in HeLa Kyoto, we could sum up to 7 frames in a 256x256 pixel image to reach 10^5 photons peak in case of an entire field of view which was necessary for fitting procedure and lifetime extraction. Cell type and signal intensity determine the optimal acquisition parameters. It is necessary to find a reasonable balance between photon number and phototoxicity and we created a troubleshooting table based on our experience (Fig 3).

Timelapse of Flipper-TR

Since the Flipper-TR probe is in dynamic exchange with the environment, measuring lifetime over time has its own challenges. If medium is added (osmotic shocks or drug addition), we advise to keep Flipper-TR concentration constant. If medium is flowed (to test the effect of shear stress for example) it is essential to keep the Flipper-TR concentration constant. Because lifetime values are broad due to inherent biological variability and impacted by cell density or cell type, we suggest assessing both lifetime variation and absolute lifetime values.

Combining Flipper probes with drug treatment

To measure the effect of a drug treatment on cells, we tested two strategies. (1) Imaging the cells, adding the drug in the medium of a dish or replacing the medium with the one that contains the drug using a microfluidic device and following the effect of the drug over time on the same cells. This approach allows to eliminate the biological variability by measuring the tension of the same cells before and after the treatment. (2) Imaging the control condition and the treated condition independently (preferably acquiring a large number of cells to increase statistics as it will be unpaired measurements, typically at least 15 fields of view per dish and 3 technical replicates). The treated cells must be imaged in the same conditions and on the same day. Since the steady state lifetime value depends on cell density, the control condition must be repeated along every drug condition with the same seeding parameters. We suggest following this strategy whenever possible. Additionally, classical solvents other than water, such as DMSO increases solution osmolarity or antibiotics used in inducible systems, such as

doxycycline, affect cholesterol amounts and therefore change the property of the membrane and affect the Flipper-TR lifetime which must be considered when designing an experiment.

Analysis

Tools to analyze the data

Several companies have made commercial packages for FLIM analysis, but these are closed source tools that are not transparent in their analyses and typically only support their own file formats. Open source and user friendly tools have been and are being developed [39,40].

Instrument response function (IRF)

To fit the signal, the contribution of the instrumentation must be isolated. The overall timing precision of a complete TCSPC system is its Instrument Response Function (IRF). The best way to measure the IRF of the system is to use a fluorophore with similar fluorescence properties as the Flipper-TR but with a very short lifetime. The IRF can be measured using fluorescein solution quenched with potassium iodide before each experiment or can be calculated (deducted) from the rising edge of the TCSPC histogram. The important point is to use the same IRF throughout the experiment. Software used to analyse FLIM images usually recalculate the IRF for each file by default, and this must be avoided to be able to compare images between them.

Photon count fitting

To extract fluorescence lifetimes, two different approaches exist: a fit-free method and an analytical method. The analytical method comprises two different models to fit the exponential decay: exponential reconvolution and exponential tailfit.

Using a fit-free method

Without going into details, the Phasor FLIM is a fit-free method which is rapid, quantitative, independent from initial conditions necessary for an exponential fit and requires less expertise in analysis. A phasor plot is generated by Fourier transform of the decay where each pixel in the image corresponds to a point in the phasor plot, rather than attempting to fit the fluorescence decay using exponential functions. This approach has the advantage to directly see if a fluorophore has a single or a multi exponential component. In the case of a multiexponential component, the ratio of their linear combination allows for direct determination of the fraction of the different lifetimes. Phasor FLIM is implemented on LEICA systems and can be for example used to quickly extract the lifetimes of different structures on one image or to separate different molecular species.

Using a tailfit model

The tailfit model consist of a multi-exponential fit applied to the region of the photon count histogram where there is no further sample excitation, (e.g where the initial exciting light pulse has dissipated). The tailfit model is particularly appropriate when examining samples with decay times significantly longer than the IRF. The choice of the fitting range is critical, users are therefore encouraged to make informed adjustments based on their specific data analysis needs.

Using a reconvolution model

The reconvolution model is a fitting procedure using a multi-exponential decay reconvoluted with the IRF. In most cases, a reconvolution fit is recommended as it allows for a complete fitting of the photon histogram. A reconvolution model requires less prior knowledge to be used than the tailfit model. However, when a sufficient number of photons are acquired, the choice between a tailfit or a reconvolution model is unlikely to significantly affect the measurement results. Tens of thousands of photons per pixel are required to accurately fit a bi-exponential decay [41].

Parameters and outputs of the multi-exponential decay for Flippers probes

Lifetime histograms of Flippers are not well fitted by a mono-exponential, but fit well toa double exponentials. By fitting with a bi-exponential decay, two lifetimes will be extracted: τ_1 and τ_2. τ_{AVG} is an average between the two rates τ_1 and τ_2 weighted by the number of photons fitted by each parameter. τ_1 (the longest component, usually ~80% of photons with a lifetime around 5.5 ns for Flipper-TR at the plasma membrane in HeLa) usually represent much higher photon counts than τ_2 (usually ~20% of photons with a lifetime around 1ns for Flipper-TR at the plasma membrane in HeLa). Both τ_1 or τ_{AVG} will directly report the mechanical property (while the fluctuation of τ_2 will be less pronounced) of the probe so you should anyway take either τ_{AVG} or the longest τ (τ_1 on picoquant system) value to analyse tension variations. In experiments analyzing the dynamics of Flipper, if the tendency of τ_1 and τ_{AVG} are different, probably because of a lack of photons, the fit and image acquisition must be optimized.

Auto-fluorescence and fluorescence lifetime of Flippers

The autofluorescence lifetime value in mammalian cells is between 1-2 ns while the Flippers lifetime is in a 4-6 ns range. Additionally, the number of photons coming from autofluorescence (from 1 to 5 photons per pixels) is negligible in comparison to the number of photons coming from the probe (around 30-100 photons per pixel depending on the laser intensity). Taken together, the autofluorescence lifetime is totally removed from τ_1 and constitute a minor contribution for $\tau_{AVG.}$

Choosing the region of interest for the tailfit and the reconvolution model

The exponential fitting can be done on a different set of pixels. The choice depends on the quality of the signal and the sensitivity of the effect targeted. (1) Whole photons analysis (which means analyzing all the photons of the image) is the simplest and necessitate little requirement of input from the experimentalist, therefore increasing the reproducibility of the work. (2) It is possible to apply a threshold on pixel intensity to remove the backound and only fit the corresponding pixels. It is however invalid to apply a threshold based on the lifetime values to select pixels from which lifetime will be extracted. Although applying a threshold on the absolute lifetime value can be used to create masks and separate objects with different Flipper lifetimes. For example, the lifetime of the plasma membrane is much higher than the lifetime of endosomal membrane, so a single FLIM image could be sufficient to discriminate the two types of objects. Similarly, it is possible to overlap a mask generated from another channel to only select pixels of interest.

Caveats for photon count fitting

Depending on the orientation of the cells in the beam, the number of photons can change (Extended Data Figure 2). A side acquisition will give a lower number of photons than an acquisition from the bottom, leading to a weaker fit (Fig 4a-c). As can be noticed from the intensity images and quantification (Extended Data Figure 2 a, e, d, h), Flipper-TR exhibit

fluorescence anisotropy when excited with linearly polarized light. This effect can be misleading for probes like Laurdan that use fluorescence intensity to report on membrane properties[42]. While the fluorescence anisotropy can lead to bright edges of vesicles or membranes aligning or misaligning with the polarization, fluorescence lifetime measurements and fitting (given enough photons are acquired) is not significantly different between bright and dark regions (Extended Data Figure 2 c, g) and can robustly report on the membrane properties. Note that the effect is stronger for membranes with higher viscosity (larger cholesterol content). However, the fluorescence anisotropy can be misleading when using intensity-weighted lifetime representations (as in FastFLIM).

Image segmentation to extract Flipper lifetime

In this section, we provide two examples to illustrate the importance of extracting the lifetime information correctly. By applying a threshold on pixel intensity, a mask can be used solely to extract lifetime of the pixels present in the mask (Fig 4d). Even if the lifetime of the internalized probe is lower than the lifetime of the probe at the plasma membrane, applying a threshold based on lifetime value will introduce a bias in the analysis of the overall lifetime. Considering only pixels corresponding to the plasma membrane instead of all the pixels of the image, which include signal coming from endosomes, gives a difference of 0.5 ns on average (Fig 4e).

The second example is illustrated by measuring the impact of blebbistatin (myosin inhibitor reducing cell contractility) on plasma membrane tension reported by Flipper-TR lifetime (Fig 4f). If all the pixels of the images (control versus blebbistatin-treated cells) are included for the fitting, a decrease of lifetime of 0.3 ns is observed (Fig 4g). Each dots represent a field of view containing several cells, the fitting was performed by fitting all the pixels. However, it appears that on images of blebbistatin-treated cells, despite an identical Flipper-TR incubation time, many intracellular membranes with a low lifetime around 2.5 ns are visible. These pixels likely contribute to the overall lower lifetime measured for blebbistatin-treated cells. By contrast, if only plasma membrane lifetime is measured, by selecting the plasma membrane pixels, the average lifetime of blebbistatin-treated cells is 0.1 ns higher than the average lifetime of control cells. Directly selecting the plasma membrane pixels also excludes the background, which could affect the analysis.

Comparing different areas within the same image

The goal of the experiments might be to compare regions within the same image. As explained above, a minimum number of photons will be necessary to obtain a decent fit and to extract the lifetime properly. Therefore, we strongly suggest checking that the photon count is similar between different area analyzed.

Anticipated results using Flipper probes

Different lifetime along cell height

By imaging Flipper-TR over z-stacks of MDCK polarized tissues, a lower lifetime (4.6 ns) at the basal plane of the cell compared to the apical plane (5.4 ns) is observed, as illustrated in Fig 5a. Also, large variability exists between position in the dish: the basal plane lifetime values vary from 4.2 ns to 5.1 ns, while the apical plane values vary between 4.3 ns and 5.6 ns. However, the lifetime of the apical plane is reproducibly higher than of the basal plane (Fig 5b) which could be explained by the known differences in lipid compositions. Therefore, single plane imaging of cells to compare, for example, different treatments, must be performed at a

similar height (Fig 5c), and sufficient statistics to account for large biological differences between single cells are required.

Mitotic cells have a more disordered plasma membrane

We analyzed the Flipper-TR lifetime in mitotic cells which are known to have a larger volume, higher cortical tension and a very different shape than adherent cells[43–45]. Mitotic cells were identified by eye based on their rounded shape and their limited attached surface to the glass bottom. We found that mitotic cells have a 0.35 ns lower lifetime (Fig 5d) compared to adherent cells[44,45], while one might have expected an increase of Flipper-TR lifetime. This lower lifetime could reflect a change of lipid composition during cell division[46], itself causing increased membrane fluidity in mitotic cells[47].

Flipper-TR variability depends on cell confluency

We analyzed the Flipper-TR lifetime depending on cell confluency. Using RPE1 cells, we observed that confluent cells have a Flipper-TR lifetime centered around 5.5 +/- 0.1 ns while non-confluent cells lifetime is centered around 5.4 +/- 0.2 ns (Fig. 5e). Interestingly, the standard deviation of the Flipper-TR lifetime is higher in cells with a lower confluency suggesting that confluency impact the cell-to-cell variability. Therefore, in case of experiments performed using cells at low confluency, larger statistics are required to account for large biological differences between single cells.

Distinguishing the contributions of lipid composition and tension to the changes of lifetime

Previous work [8] showed that mechanical increase of GUVs composed of DOPC:SM:CL 30:30:40) membrane tension induced by micropipette aspiration (high tension) leads to an increase of 0.2 ns of Flipper-TR lifetime (8). Using the same setup to aspirate HeLa cells in suspension (Fig 5f), an increase of 0.2 ns was also observed (Fig 5g), confirming that in both GUVs and cells Flipper-TR lifetime measurements can directly report a mechanically induced change of membrane tension.

Although being slightly lower than Flipper (steady state lifetime of 5.0 ns vs 5.8 ns for SM/Chol GUV), the lifetime of super-resolution (SR)-Flipper also reports changes in membrane tension of GUVs (Fig 6a-b) as well as changes in lipid composition. SR-Flipper-TR lifetime of SM/Chol (70/30) GUV is centered around 5 ns while the lifetime of DOPC/Chol (70/30) GUV is centered around 4.2 ns (Fig 6b). With both lipid compositions, SR-Flipper lifetime decreases upon membrane tension decrease induced by hypertonic shocks proving that Flipper probes lifetime report both lipid composition and membrane tension (Fig 6a-e). In contrast, the lifetime of pure DOPC GUVs is not changing after hypertonic shock which is in good agreement with an absence of phase separation (Fig 6a, f).

Niemann-Pick C1 protein (NPC1) is responsible of the intracellular transport of Cholesterol and sphingolipids. Consequently, the depletion of NPC1 is responsible for cholesterol accumulation in endosomes. Consistently, LysoFlipper in HeLa MZ NPC1 KO cells have a higher lifetime than in WT HeLa cells indicating higher lipid packing (Fig 6g, h). Nonetheless, the probe is still able to report a change in membrane tension, as demonstrated by lifetime decrease under hypertonic treatment (Fig 6g, i).

The protein Cavin1 is a major component of caveolae and its deletion prevents caveolae assembly[10,48]. Interestingly, the absence of caveolae in Cavin1-KO cells is associated with a smaller Flipper-TR lifetime, indicating either a lower membrane tension or a more disordered membrane composition (Fig 6j, k). Cavin1-KO cells show a lifetime increase upon hypotonic shocks (Fig 6j, l). Thus, despite a potential difference of lipid composition, Flipper-TR is anyway able to report an increase of membrane tension.

Conclusions

Here, we have reported the current technical capabilities of using Flipper probes, and how we overcame the challenges we faced. Technical improvements in the FLIM image acquisition and analysis may help expand the use of Flipper probes to other biological samples of interest. Flipper probes remain an interesting tool for many applications, and in some cases, the only available tool to measure membrane tension.

Acknowledgments

We thank Shankar Srinivas and Christophe Royer (University of Oxford) for isolating and staining the mouse embryos. FS is grateful for the support from the EMBO (ALTF 849-2020) and HFSP (LT000404/2021-L) long-term postdoctoral fellowships. FS thanks Scott Fraser (University of Southern California) for the support and supervision and acknowledges the Translational Imaging Center (University of Southern California) for access to instrumentation and expertise. A.C. also acknowledges funding from MCIU, PID2019-111096GA-I00; MCIU/AEI/FEDER MINECOG19/P66, RYC2018-024686-I, and Basque Government T1270-19. VD thanks Pierre-François Lenne (IBDM Marseille) for supervision and resources. V.D. acknowledges support by an HFSP long-term postdoctoral fellowship (HFSP LT0058/2022-L) and the France-BioImaging infrastructure supported by the French National Research Agency (ANR–10–INBS- 04-01, Investments for the future). VD thanks Frank Schnorrer (IBDM Marseille) for access to the FLIM system. SM thank the University of Geneva, the National Centre of Competence in Research (NCCR) Chemical Biology (51NF40-185898), the NCCR Molecular Systems Engineering (51NF40-182895), and the Swiss NSF (Excellence Grant 200020 204175; SNSF-ERC Advanced Grant TIMEUP, TMAG-2_209190) for financial support. AR acknowledges funding from the Swiss National Fund for Research Grants N°310030_200793 and N°CRSII5_189996, the European Research Council Synergy Grant N° 951324 R2-TENSION.

Author contributions section

The project was designed by CR, AR and VM. CR & VM carried out most of the experiments and analyses. JMGA performed the experiments on bacteria, PC performed some experiments on MDCK, CT performed experiments on alginate tubes, FS performed the biphoton experiments, IDM performed experiments with alginate capsules, AC performed experiments on *Arabidopsis*, KB and VD performed the experiments on *Xenopus* and JLA and SM designed and synthesized the Flippers molecules. CR, VM and AR wrote the paper, with corrections from all co-authors.

Competing interests statement

The authors declare no competing interests.

Bibliography

1. Roca-Cusachs, P., Conte, V. & Trepat, X. Quantifying forces in cell biology. *Nat. Cell Biol.* **19**, 742–751 (2017).
2. Abella, M., Andruck, L., Malengo, G. & Skruzny, M. Actin-generated force applied during endocytosis measured by Sla2-based FRET tension sensors. *Dev. Cell* **56**, 2419-2426.e4 (2021).
3. Déjardin, T. *et al.* Nesprins are mechanotransducers that discriminate epithelial-mesenchymal transition programs. *J. Cell Biol.* **219**, e201908036 (2020).
4. Li, W. *et al.* A Membrane-Bound Biosensor Visualizes Shear Stress-Induced Inhomogeneous Alteration of Cell Membrane Tension. *iScience* **7**, 180–190 (2018).
5. Páez-Pérez, M., López-Duarte, I., Vyšniauskas, A., Brooks, N. J. & Kuimova, M. K. Imaging non-classical mechanical responses of lipid membranes using molecular rotors. *Chem Sci* **12**, 2604–2613 (2021).
6. Assies, L. *et al.* Flipper Probes for the Community. *Chim. Int. J. Chem.* **75**, 1004–1011 (2021).
7. Soleimanpour, S. *et al.* Headgroup engineering in mechanosensitive membrane probes. *Chem. Commun.* **52**, 14450–14453 (2016).
8. Colom, A. *et al.* A fluorescent membrane tension probe. *Nat. Chem.* **10**, 1118–1125 (2018).
9. Mercier, V. *et al.* Endosomal membrane tension regulates ESCRT-III-dependent intra-lumenal vesicle formation. *Nat. Cell Biol.* **22**, 947–959 (2020).
10. Roffay, C. *et al.* Passive coupling of membrane tension and cell volume during active response of cells to osmosis. *Proc. Natl. Acad. Sci.* **118**, (2021).
11. Ni, Q. *et al.* Cytoskeletal activation of NHE1 regulates cell volume and DNA methylation. 2023.08.31.555808 Preprint at https://doi.org/10.1101/2023.08.31.555808 (2023).
12. Michels, L. *et al.* Complete microviscosity maps of living plant cells and tissues with a toolbox of targeting mechanoprobes. *Proc. Natl. Acad. Sci.* **117**, 18110–18118 (2020).

13. Coomer, C. A. *et al.* Single-cell glycolytic activity regulates membrane tension and HIV-1 fusion. *PLOS Pathog.* **16**, e1008359 (2020).
14. Jiménez-Rojo, N. *et al.* Conserved Functions of Ether Lipids and Sphingolipids in the Early Secretory Pathway. *Curr. Biol.* **30**, 3775-3787.e7 (2020).
15. Mylvaganam, S. *et al.* The spectrin cytoskeleton integrates endothelial mechanoresponses. *Nat. Cell Biol.* **24**, 1226–1238 (2022).
16. Lachuer, H., Le, L., Lévêque-Fort, S., Goud, B. & Schauer, K. Membrane tension spatially organizes lysosomal exocytosis. 2022.04.22.489160 Preprint at https://doi.org/10.1101/2022.04.22.489160 (2022).
17. Lachowski, D. *et al.* Substrate Stiffness-Driven Membrane Tension Modulates Vesicular Trafficking via Caveolin-1. *ACS Nano* **16**, 4322–4337 (2022).
18. Riggi, M. *et al.* Decrease in plasma membrane tension triggers PtdIns(4,5)P2 phase separation to inactivate TORC2. *Nat. Cell Biol.* **20**, 1043–1051 (2018).
19. Riggi, M., Kusmider, B. & Loewith, R. The flipside of the TOR coin – TORC2 and plasma membrane homeostasis at a glance. *J. Cell Sci.* **133**, (2020).
20. Wang, S. *et al.* Adipocyte Piezo1 mediates obesogenic adipogenesis through the FGF1/FGFR1 signaling pathway in mice. *Nat. Commun.* **11**, 2303 (2020).
21. Nava, M. M. *et al.* Heterochromatin-Driven Nuclear Softening Protects the Genome against Mechanical Stress-Induced Damage. *Cell* **181**, 800-817.e22 (2020).
22. Schneider, A. F. L., Kithil, M., Cardoso, M. C., Lehmann, M. & Hackenberger, C. P. R. Cellular uptake of large biomolecules enabled by cell-surface-reactive cell-penetrating peptide additives. *Nat. Chem.* **13**, 530–539 (2021).
23. Hetmanski, J. H. R. *et al.* Membrane Tension Orchestrates Rear Retraction in Matrix-Directed Cell Migration. *Dev. Cell* **51**, 460-475.e10 (2019).

628 24. Yavitt, F. M. *et al.* In situ modulation of intestinal organoid epithelial curvature through
629 photoinduced viscoelasticity directs crypt morphogenesis. *Sci. Adv.* **9**, eadd5668 (2023).
630 25. Goujon, A. *et al.* Mechanosensitive Fluorescent Probes to Image Membrane Tension in
631 Mitochondria, Endoplasmic Reticulum, and Lysosomes. *J. Am. Chem. Soc.* **141**, 3380–
632 3384 (2019).
633 26. Dal Molin, M. *et al.* Fluorescent Flippers for Mechanosensitive Membrane Probes. *J. Am.*
634 *Chem. Soc.* **137**, 568–571 (2015).
635 27. García-Sáez, A. J., Chiantia, S. & Schwille, P. Effect of Line Tension on the Lateral
636 Organization of Lipid Membranes *. *J. Biol. Chem.* **282**, 33537–33544 (2007).
637 28. Hamada, T., Kishimoto, Y., Nagasaki, T. & Takagi, M. Lateral phase separation in tense
638 membranes. *Soft Matter* **7**, 9061–9068 (2011).
639 29. Shimokawa, N. & Hamada, T. Physical Concept to Explain the Regulation of Lipid
640 Membrane Phase Separation under Isothermal Conditions. *Life* **13**, 1105 (2023).
641 30. García-Calvo, J. *et al.* HydroFlipper membrane tension probes: imaging membrane
642 hydration and mechanical compression simultaneously in living cells. *Chem. Sci.* **13**, 2086–
643 2093 (2022).
644 31. Licari, G., Strakova, K., Matile, S. & Tajkhorshid, E. Twisting and tilting of a
645 mechanosensitive molecular probe detects order in membranes. *Chem. Sci.* **11**, 5637–5649
646 (2020).
647 32. Harris, F. M., Best, K. B. & Bell, J. D. Use of laurdan fluorescence intensity and
648 polarization to distinguish between changes in membrane fluidity and phospholipid order.
649 *Biochim. Biophys. Acta* **1565**, 123–128 (2002).
650 33. Golfetto, O., Hinde, E. & Gratton, E. Laurdan fluorescence lifetime discriminates
651 cholesterol content from changes in fluidity in living cell membranes. *Biophys. J.* **104**,
652 1238–1247 (2013).

34. Ragaller, F. *et al.* Quantifying fluorescence lifetime responsiveness of environment sensitive probes for membrane fluidity measurements. 2023.10.23.563572 Preprint at https://doi.org/10.1101/2023.10.23.563572 (2023).
35. Piazzolla, F. *et al.* Fluorescent Membrane Tension Probes for Early Endosomes. *Angew. Chem.* **133**, 12366–12371 (2021).
36. Royer, C. *et al.* ASPP2 maintains the integrity of mechanically stressed pseudostratified epithelia during morphogenesis. *Nat. Commun.* **13**, 941 (2022).
37. García-Calvo, J. *et al.* Fluorescent Membrane Tension Probes for Super-Resolution Microscopy: Combining Mechanosensitive Cascade Switching with Dynamic-Covalent Ketone Chemistry. *J. Am. Chem. Soc.* **142**, 12034–12038 (2020).
38. López-Andarias, J. *et al.* Photocleavable Fluorescent Membrane Tension Probes: Fast Release with Spatiotemporal Control in Inner Leaflets of Plasma Membrane, Nuclear Envelope, and Secretory Pathway. *Angew. Chem. Int. Ed.* **61**, e202113163 (2022).
39. Gao, D. *et al.* FLIMJ: An open-source ImageJ toolkit for fluorescence lifetime image data analysis. *PLOS ONE* **15**, e0238327 (2020).
40. Warren, S. C. *et al.* Rapid Global Fitting of Large Fluorescence Lifetime Imaging Microscopy Datasets. *PLOS ONE* **8**, e70687 (2013).
41. Köllner, M. & Wolfrum, J. How many photons are necessary for fluorescence-lifetime measurements? *Chem. Phys. Lett.* **200**, 199–204 (1992).
42. Parasassi, T., Gratton, E., Yu, W. M., Wilson, P. & Levi, M. Two-photon fluorescence microscopy of laurdan generalized polarization domains in model and natural membranes. *Biophys. J.* **72**, 2413–2429 (1997).
43. Zlotek-Zlotkiewicz, E., Monnier, S., Cappello, G., Le Berre, M. & Piel, M. Optical volume and mass measurements show that mammalian cells swell during mitosis. *J. Cell Biol.* **211**, 765–774 (2015).

678 44. Fischer-Friedrich, E., Hyman, A. A., Jülicher, F., Müller, D. J. & Helenius, J.
679 Quantification of surface tension and internal pressure generated by single mitotic cells.
680 *Sci. Rep.* **4**, 1–8 (2014).
681 45. Stewart, M. P. *et al.* Hydrostatic pressure and the actomyosin cortex drive mitotic cell
682 rounding. *Nature* **469**, 226–230 (2011).
683 46. Storck, E. M., Özbalci, C. & Eggert, U. S. Lipid Cell Biology: A Focus on Lipids in Cell
684 Division. *Annu. Rev. Biochem.* **87**, 839–869 (2018).
685 47. Atilla-Gokcumen, G. E. *et al.* Dividing cells regulate their lipid composition and
686 localization. *Cell* **156**, 428–439 (2014).
687 48. Andrade, V. *et al.* Caveolae promote successful abscission by controlling intercellular
688 bridge tension during cytokinesis. *Sci. Adv.* **8**, eabm5095.
689

Captions:

Figure 1: Principles of Flipper probe

(a) Flipper design is a planar push-pull system. Mechanical planarization is responsible for a spectrum of configurations from planar to twisted configuration, which will affect the photo-physics and notably the time of the excited state of the probe

(b) Lateral forces within the membrane directly set the twisting and therefore the photo-physics of the Flipper probes.

(c) In complex membranes (e.g cell membranes), high tensile stress will trigger phase separation and the formation of highly packed membrane nanodomains reported by an increase of Flippers lifetime.

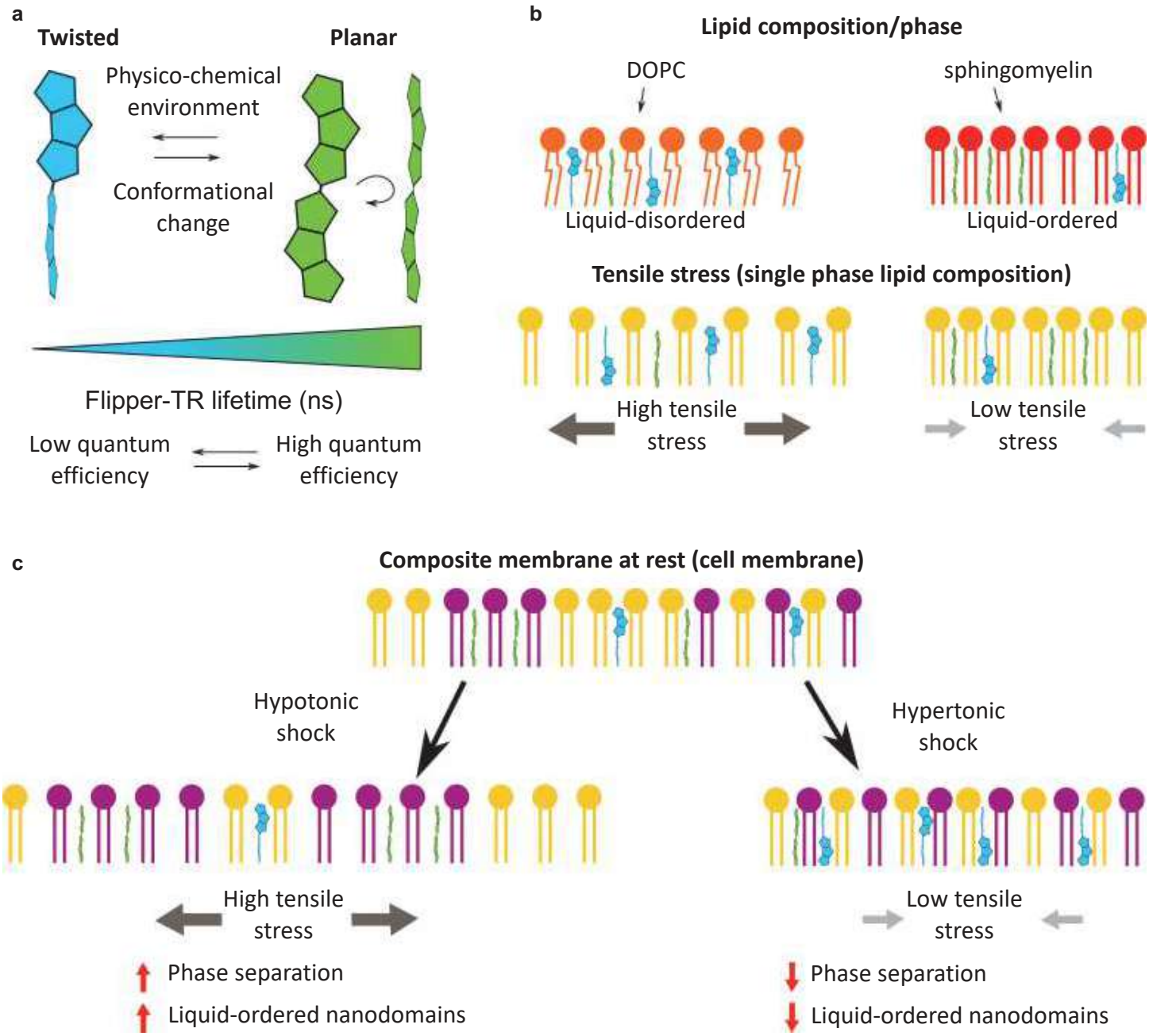
a
Twisted
Planar
Physico-chemical environment
Conformational change
Flipper-TR lifetime (ns)
Low quantum efficiency
High quantum efficiency
b
Lipid composition/phase
DOPC
sphingomyelin
Liquid-disordered
Liquid-ordered
Tensile stress (single phase lipid composition)
High tensile stress
Low tensile stress
c
Composite membrane at rest (cell membrane)
Hypotonic shock
Hypertonic shock
High tensile stress
Low tensile stress
Phase separation
Liquid-ordered nanodomains
Phase separation
Liquid-ordered nanodomains

Figure 2: General behavior of Flipper probes

(a) Graph showing the Flipper-TR lifetime (τ_1) extracted from different cell types. The different cell types used are detailed in the Methods section.

(b) Graph showing the Endo Flipper lifetime (τ_1) extracted from different cell types (n>5 field of view with at least 5 cells per field for each condition)

(c) Graph showing the Lyso Flipper lifetime (τ_1) extracted from different cell types (n>5 fields of view with at least 5 cells per field for each condition)

(d) FLIM images showing MDCK tissue stained with Flipper-TR at different timepoints. Scale bar: 80 μm.

(e) Flipper-TR FLIM and confocal image of HeLa cells labelled with Flipper-TR lifetime and smURFP fluorescence. Scale bar: 30 μm.

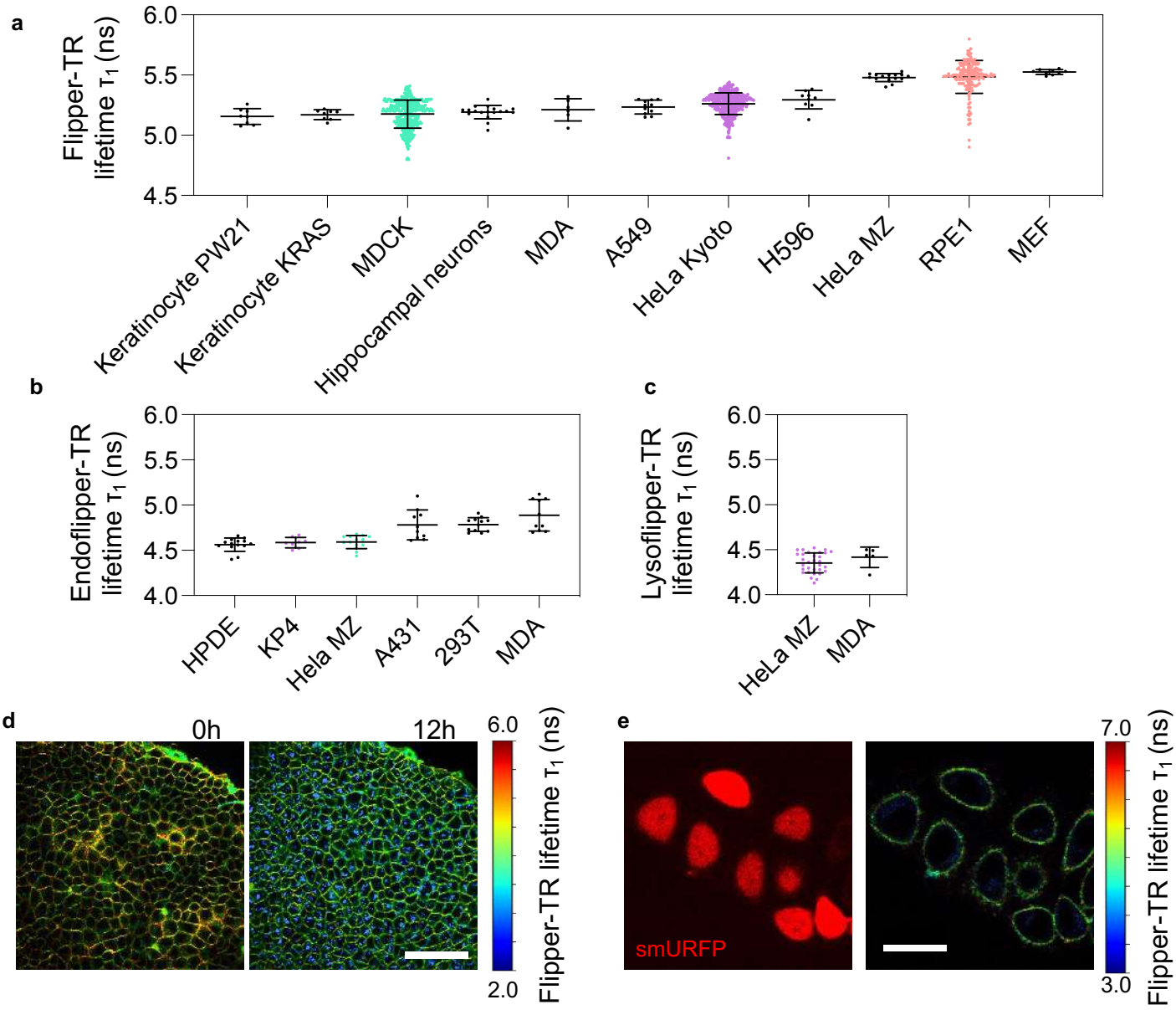
a
Flipper-TR lifetime τ1 (ns)
6.0
5.5
5.0
4.5
Keratinocyte PW21
Keratinocyte KRAS
MDCK
Hippocampal neurons
MDA
A549
HeLa Kyoto
H596
HeLa MZ
RPE1
MEF
b
Endoflipper-TR lifetime τ1 (ns)
6.0
5.5
5.0
4.5
4.0
HPDE
KP4
Hela MZ
A431
293T
MDA
c
Lysoflipper-TR lifetime τ1 (ns)
6.0
5.5
5.0
4.5
4.0
HeLa MZ
MDA
d
0h
12h
6.0
2.0
Flipper-TR lifetime τ1 (ns)
e
smURFP
7.0
3.0
Flipper-TR lifetime τ1 (ns)

Figure Box 1: Flipper probes staining in various model and organisms

(a) Representative fluorescence image of a MDCK monolayer in an alginate capsule (Myr-Palm-GFP stain the MDCK cells and ATTO647 stain the alginate capsule in blue) on the left and a representative FLIM image of an MDCK monolayer stained with Flipper-TR in an alginate capsule. Scale bar is 50 μm.

(b) Representative FLIM bottom view of an MDCK monolayer stained with Flipper-TR in an alginate tube. Scale bar is 20 μm.

(c) Representative FLIM side view of an MDCK monolayer stained with Flipper-TR in a PDMS roll. Scale bar is 20 μm.

(d) Representative FLIM image of Arabidopsis root and of the entire Arabidopsis embryo stained with Flipper-TR. Scale bar is 20 μm for the left panel and 40 μm for the right panel.

(e) Representative FLIM image of Arabidopsis leaf and of Arabidopsis root stained with Flipper-TR. Scale bar are 20 μm.

(f) Representative FLIM image of Xenopus explant stained with Flipper-TR. Scale bar is 100 μm.

(g) Representative FLIM image of mESC gastruloid stained with Flipper-TR. Scale bar is 80 μm.

(h) Representative FLIM image in E6.5 mouse embryos stained with Flipper-TR. Scale bar is 20 μm.

(i) Top: representative FLIM image of Gram-negative (E. coli) stained with Flipper-TR showing a non-specific signal and its corresponding zoom in on the right. Bottom: representative FLIM image of Gram-positive (B. subtilis) stained with Flipper-TR and and its corresponding zoom in on the right. Scale bar is 10 μm for left images and 3 μm for right images.

(j) Quantification of the number of photons per pixel of Gram-negative (E. coli) and Gram-positive (B. subtilis)

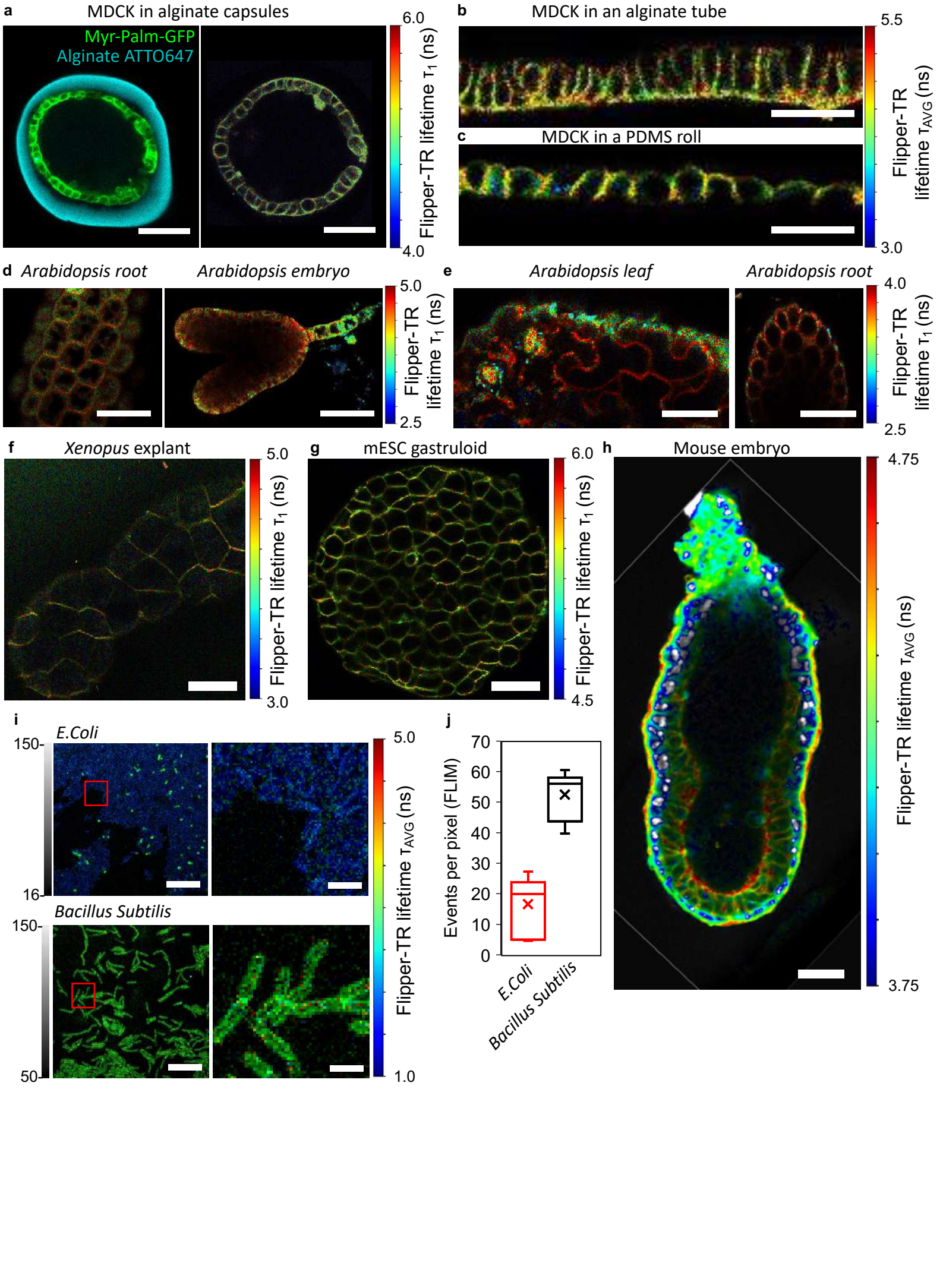
a
MDCK in alginate capsules
Myr-Palm-GFP
Alginate ATTO647
6.0
4.0
Flipper-TR lifetime τ1 (ns)
b
MDCK in an alginate tube
c
MDCK in a PDMS roll
5.5
3.0
Flipper-TR lifetime τAVG (ns)
d
Arabidopsis root
Arabidopsis embryo
5.0
2.5
Flipper-TR lifetime τ1 (ns)
e
Arabidopsis leaf
Arabidopsis root
4.0
2.5
Flipper-TR lifetime τ1 (ns)
f
Xenopus explant
5.0
3.0
Flipper-TR lifetime τ1 (ns)
g
mESC gastruloid
6.0
4.5
Flipper-TR lifetime τ1 (ns)
h
Mouse embryo
4.75
3.75
Flipper-TR lifetime τAVG (ns)
i
E.Coli
150
16
Bacillus Subtilis
150
50
5.0
1.0
Flipper-TR lifetime τAVG (ns)
j
Events per pixel (FLIM)
70
60
50
40
30
20
10
0
E.Coli
Bacillus Subtilis

Figure 3: Troubleshooting Flipper probes experiments. This table shows the different issues that can be encountered, where the limitations come from and how they can be solved.

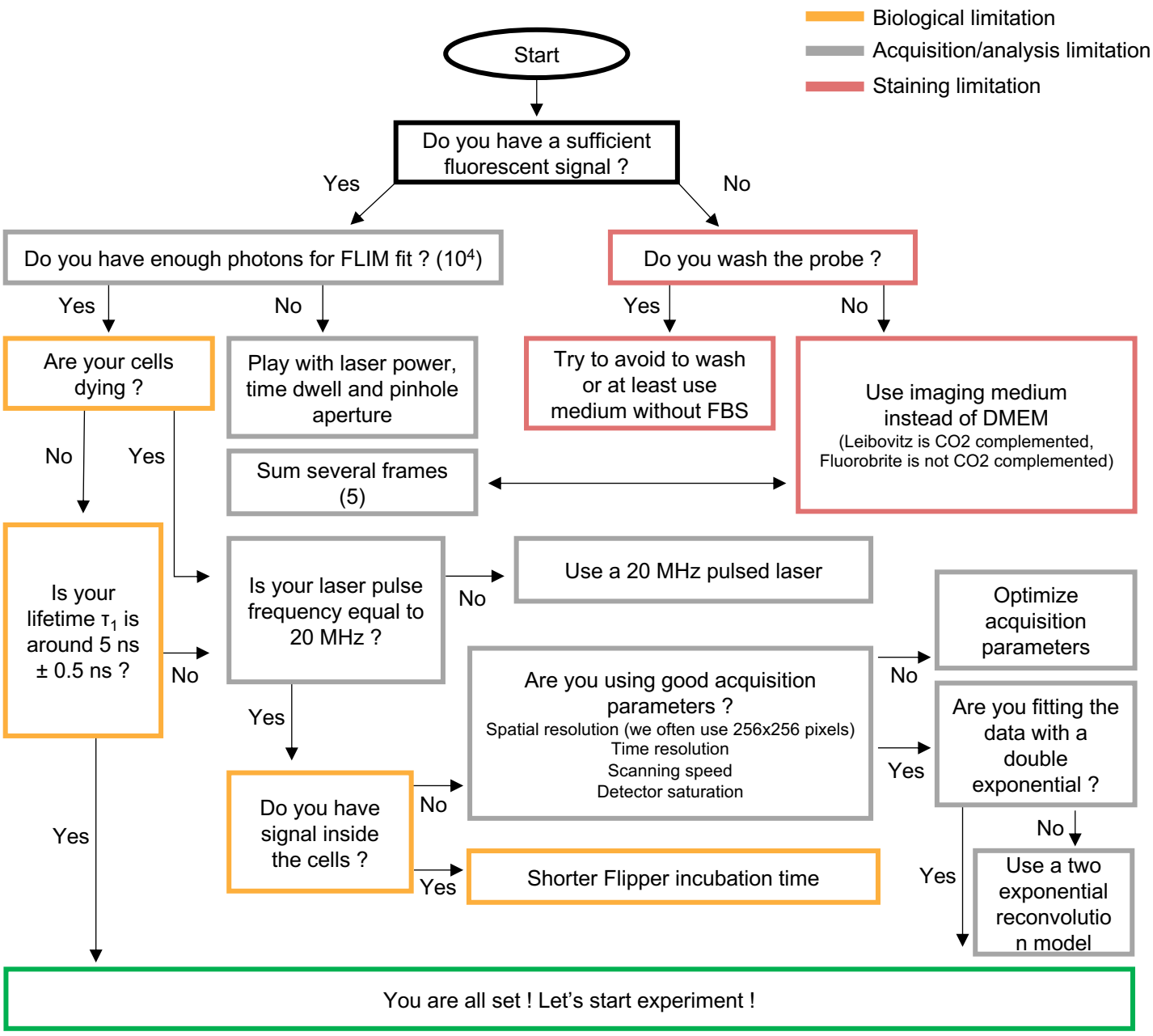
Biological limitation
Acquisition/analysis limitation
Staining limitation
Start
Do you have a sufficient fluorescent signal ?
Yes
No
Do you have enough photons for FLIM fit ? (10⁴)
Do you wash the probe ?
Yes
No
Yes
No
Are your cells dying ?
Play with laser power, time dwell and pinhole aperture
Try to avoid to wash or at least use medium without FBS
Use imaging medium instead of DMEM
(Leibovitz is CO2 complemented, Fluorobrite is not CO2 complemented)
Sum several frames (5)
No
Yes
Is your lifetime τ1 is around 5 ns ± 0.5 ns ?
Is your laser pulse frequency equal to 20 MHz ?
Use a 20 MHz pulsed laser
No
Optimize acquisition parameters
No
Are you using good acquisition parameters ?
Spatial resolution (we often use 256x256 pixels)
Time resolution
Scanning speed
Detector saturation
Are you fitting the data with a double exponential ?
Yes
Yes
No
Do you have signal inside the cells ?
No
Yes
Shorter Flipper incubation time
Yes
No
Use a two exponential reconvolution model
You are all set ! Let's start experiment !

Figure 4: How to properly extract the Flipper-TR lifetime from FLIM image.
(a) Representative FLIM images of MDCK tissue in PDMS roll stained with Flipper-TR acquired from the side (top row) or from the bottom (bottom row). Scale bar is 40 μm.
(b) Graph showing the Flipper-TR lifetime (τ_1, ns) extracted from the pixels of the side acquisition image versus from the bottom acquisition image.
(c) Graph showing the number of photons extracted from the pixels of the side acquisition image versus from the bottom acquisition image.
(d) Representative FLIM images of MDCK tissue stained with Flipper-TR (top row) with and without endosomal staining (respectively top panel and bottom panel after 8h of incubation) due to longer cell incubation with Flipper-TR. Flipper-TR lifetime of pixels corresponding only to plasma membrane (PM) extracted via the segmentation of the PM (middle column) based on Flipper-TR fluorescence intensity. Scale bar is 40 μm.
(e) Graph showing the Flipper-TR lifetime (τ_1, ns) extracted from all the pixels of the image versus only the pixels corresponding to the plasma membrane.
(f) Representative FLIM images of HeLa cells incubated with DMSO (top) or with 10 uM blebbistatin preincubated in DMEM at 37 °C for 45 min and kept constant throughout the experiment (bottom). Bottom images show two configurations: all the pixels are selected (left) or only pixels corresponding to PM were manually selected (right). Scale bar is 40 μm.
(g) Graph showing Flipper-TR lifetime quantification corresponding to (f). Lifetime (τ_1, ns) was extracted from all the pixels of the image versus only the pixels corresponding to the plasma membrane (n=30 field of view for both control and blebbistatin treated cells)

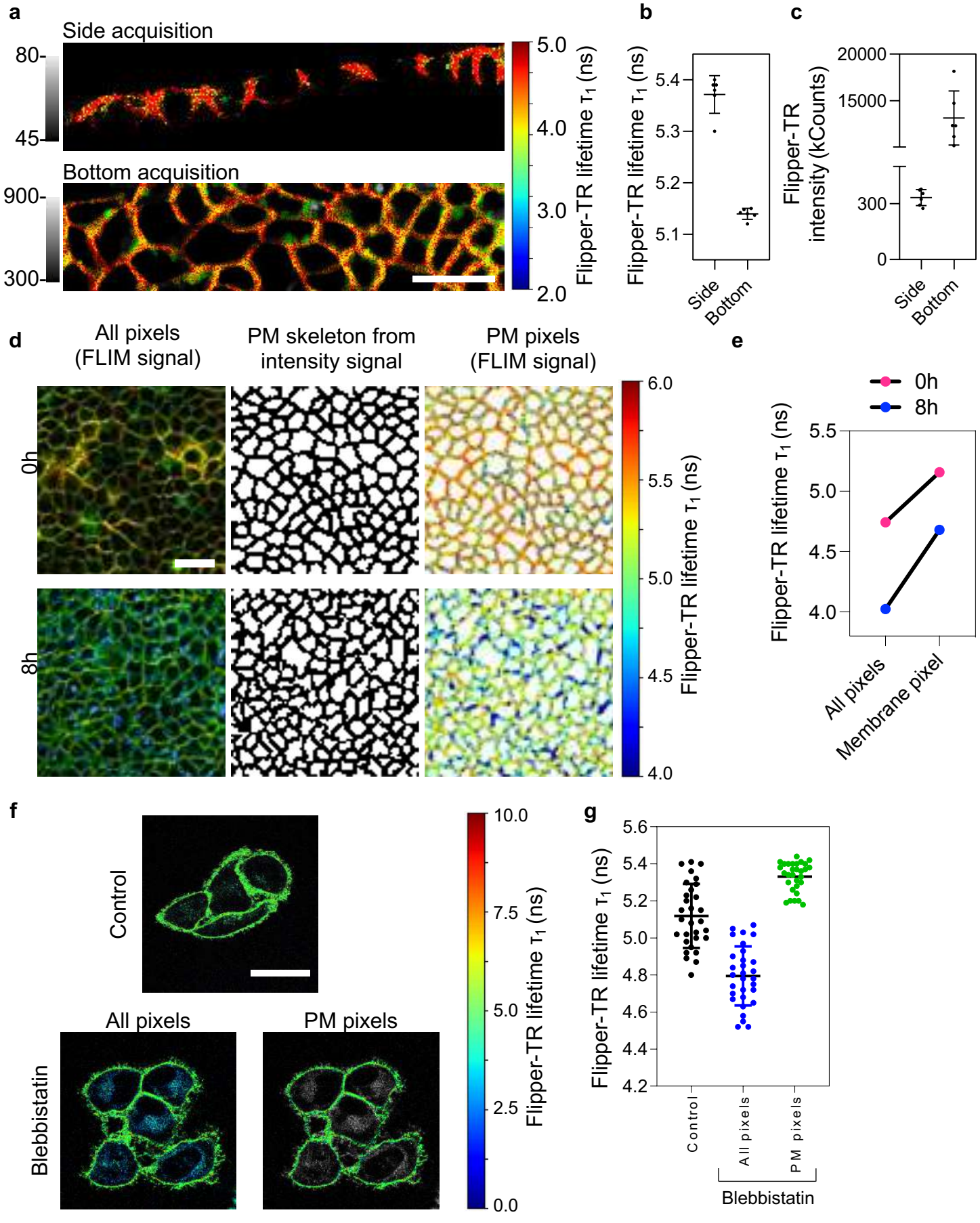
a
Side acquisition
80
45
Bottom acquisition
900
300
5.0
4.0
3.0
2.0
Flipper-TR lifetime τ1 (ns)
b
Flipper-TR lifetime τ1 (ns)
5.4
5.3
5.2
5.1
Side
Bottom
c
Flipper-TR intensity (kCounts)
20000
15000
300
0
Side
Bottom
d
All pixels (FLIM signal)
PM skeleton from intensity signal
PM pixels (FLIM signal)
0h
8h
6.0
5.5
5.0
4.5
4.0
Flipper-TR lifetime τ1 (ns)
e
0h
8h
Flipper-TR lifetime τ1 (ns)
5.5
5.0
4.5
4.0
All pixels
Membrane pixel
f
Control
All pixels
PM pixels
Blebbistatin
10.0
7.5
5.0
2.5
0.0
Flipper-TR lifetime τ1 (ns)
g
Flipper-TR lifetime τ1 (ns)
5.6
5.4
5.2
5.0
4.8
4.6
4.4
4.2
Control
All pixels
PM pixels
Blebbistatin

Figure 5: Flipper-TR lifetime is affected by several parameters

(a) Representative FLIM images of MDCK tissue stained with Flipper-TR in the apical plan (top row) ant the basal plan (bottom row). Scale bar is 40 μm.

(b) Graph showing the quantification of Flipper-TR lifetime (ns) in the apical plane (4.0 micron from the bottom) and the basal plane (1.2 micron from the bottom). The bottom was determined as the plane with the highest number of photons (n = 45).

(c) Graph showing the quantification of Flipper-TR lifetime (τ_1, ns) from the bottom plane to the apical plane by steps of 0.4 micron. Each curve represents the lifetime of an entire field of view (n = 45).

(d) Graph showing the quantification of Flipper-TR lifetime (τ_1, ns) in mitotic and non-mitotic HeLa cells

(e) Graph showing the quantification of Flipper-TR lifetime (τ1, ns) in confluent and non-confluent RPE1 cells

(f) Representative Flipper-TR FLIM images of HeLa cell aspirated in a micropipette at different aspiration pressure. Scale bar: 10 μm

(g) Graph showing the quantification corresponding to (c) of Flipper-TR lifetime (τ_1, ns) depending on the aspiration pressure applied to the cell.

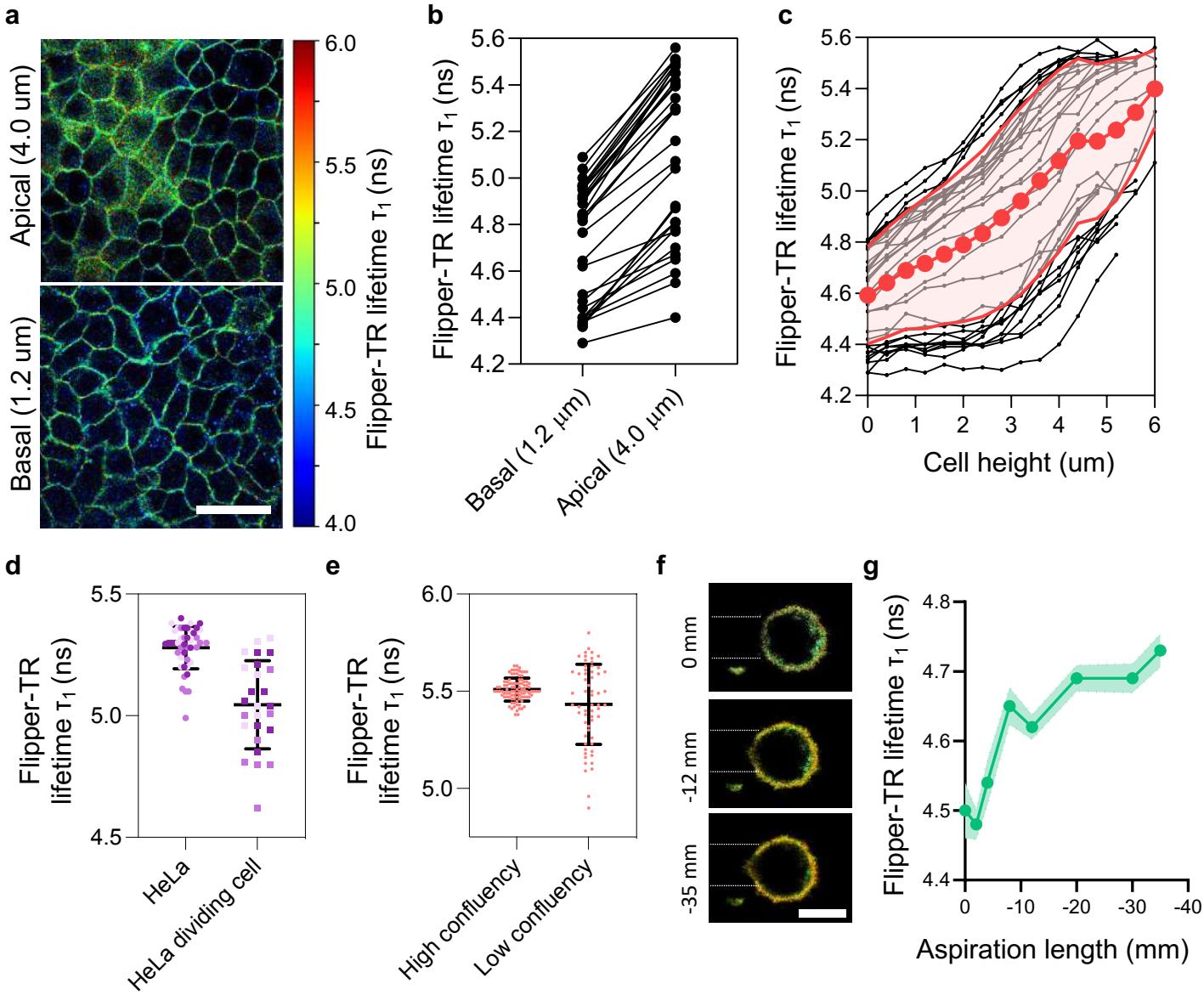
a
Apical (4.0 um)
Basal (1.2 um)
6.0
5.5
5.0
4.5
4.0
Flipper-TR lifetime τ1 (ns)
b
Flipper-TR lifetime τ1 (ns)
5.6
5.4
5.2
5.0
4.8
4.6
4.4
4.2
Basal (1.2 µm)
Apical (4.0 µm)
c
Flipper-TR lifetime τ1 (ns)
Cell height (um)
0
1
2
3
4
5
6
d
Flipper-TR lifetime τ1 (ns)
5.5
5.0
4.5
HeLa
HeLa dividing cell
e
Flipper-TR lifetime τ1 (ns)
6.0
5.5
5.0
High confluency
Low confluency
f
0 mm
-12 mm
-35 mm
g
Flipper-TR lifetime τ1 (ns)
4.8
4.7
4.6
4.5
4.4
0
-10
-20
-30
-40
Aspiration length (mm)

Figure 6: Flipper lifetime allow to detect membrane tension variations although if lipid composition is different.

(a) Representative FLIM images before and after hypertonic shocks of SM/Chol containing GUVs stained with Flipper-TR or SR-Flipper, DOPC/Chol containing GUVs stained with SR-Flipper and of DOPC containing GUVs stained with SR-Flipper. Scale bar is 50 μm.

(b) Graph showing the quantification of Flipper-TR and SR-Flipper lifetime (τ_1, ns) before hypertonic shock on GUV of specified lipid composition.

(c) Graph showing the quantification of Flipper-TR lifetime (τ_1, ns) before and after hypertonic shock on SM/Chol GUV.

(d-f) Graph showing the quantification of SR-Flipper lifetime (τ_1, ns) before and after hypertonic shock on GUV of specified lipid composition.

(g) Top: representative Endo Flipper FLIM images of HeLa MZ cells (left) and HeLa MZ NPC1 KO cells (right), which present accumulation of Cholesterol in endosomes. Bottom: representative Endo Flipper FLIM images of HeLa MZ NPC1 KO cells before hypertonic shock (left) and after hypertonic shock (right). Scale bar is 4 μm.

(h) Graph showing the quantification of Endo Flipper lifetime (ns) of HeLa MZ cells and HeLa MZ NPC1 KO cells in isotonic condition.

(i) Graph showing the quantification of Endo Flipper lifetime (τ_1, ns) before and after hypertonic shock

(j) Representative Flipper-TR FLIM images of HeLa Cavin1-KO cells before hypotonic shock (left) and after hypotonic shock (right). Scale bar is 40 μm.

(k) Graph showing the quantification of Flipper-TR lifetime (τ_1, ns) in HeLa cells (n = 10) and HeLa Cavin1-KO cells (n = 10) in isotonic medium.

(l) Graph showing the quantification of Flipper-TR lifetime (τ_1, ns) in HeLa Cavin1-KO cells (n = 4) after a hypotonic shock.

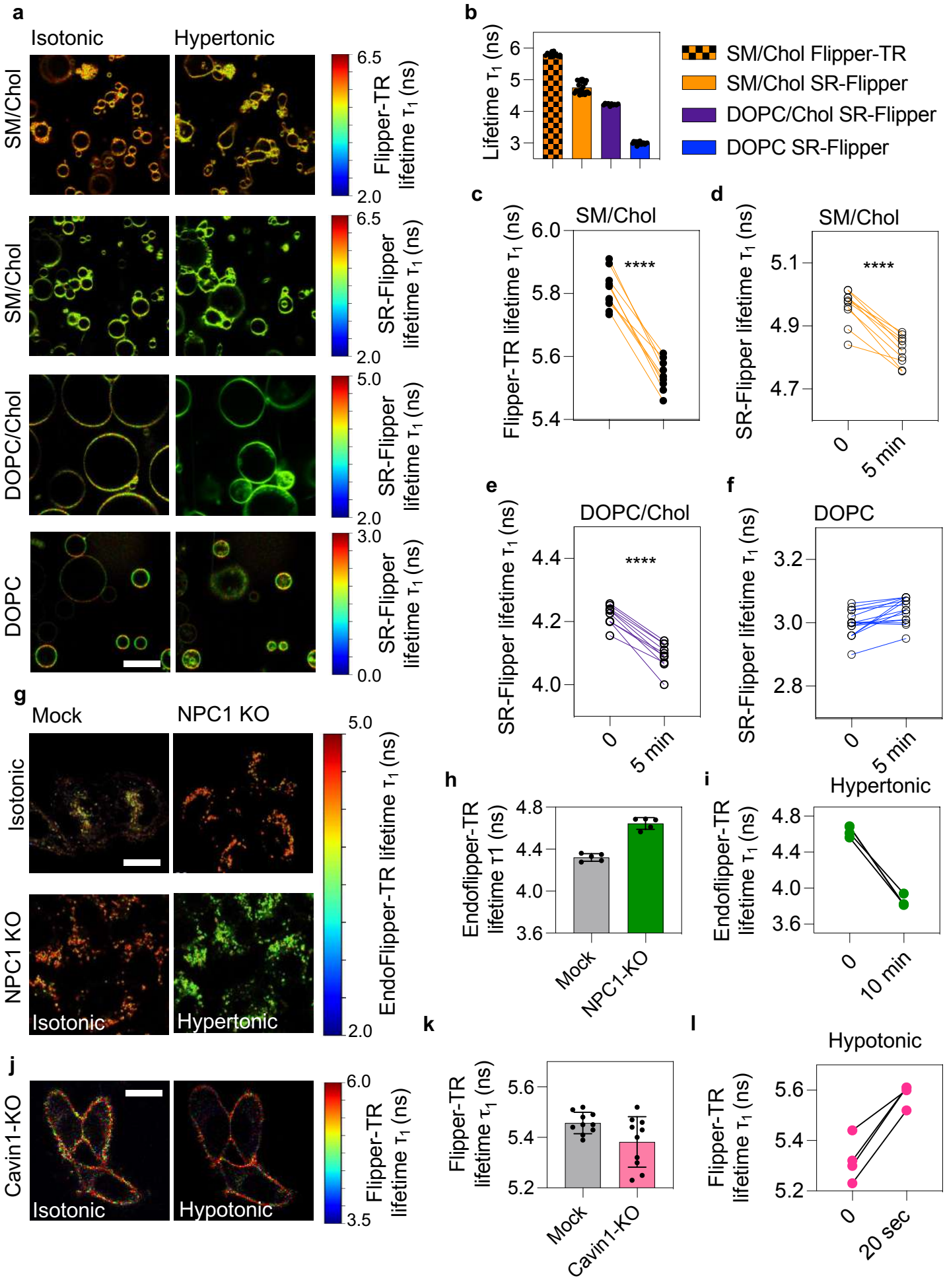
a
Isotonic
Hypertonic
SM/Chol
SM/Chol
DOPC/Chol
DOPC
Flipper-TR lifetime τ1 (ns)
SR-Flipper lifetime τ1 (ns)
b
Lifetime τ1 (ns)
SM/Chol Flipper-TR
SM/Chol SR-Flipper
DOPC/Chol SR-Flipper
DOPC SR-Flipper
c
SM/Chol
Flipper-TR lifetime τ1 (ns)
****
d
SM/Chol
SR-Flipper lifetime τ1 (ns)
****
0
5 min
e
DOPC/Chol
SR-Flipper lifetime τ1 (ns)
****
f
DOPC
SR-Flipper lifetime τ1 (ns)
g
Mock
NPC1 KO
Isotonic
NPC1 KO
Isotonic
Hypertonic
EndoFlipper-TR lifetime τ1 (ns)
h
Endoflipper-TR lifetime τ1 (ns)
Mock
NPC1-KO
i
Hypertonic
Endoflipper-TR lifetime τ1 (ns)
0
10 min
j
Cavin1-KO
Isotonic
Hypotonic
Flipper-TR lifetime τ1 (ns)
k
Flipper-TR lifetime τ1 (ns)
Mock
Cavin1-KO
l
Hypotonic
Flipper-TR lifetime τ1 (ns)
0
20 sec

Extended Data Figure 1: FLIM of Flipper-TR using two-photon microscopy

(a) Absorption and excitation spectrum of the Flipper-TR.

(b) Two-photon excitation spectra of Flipper-TR, acquired in 48h gastruloids. Five gastruloids were imaged in total at each wavelength. The acquired spectra were normalized to the maximum intensity value. Dots represented the average value, scattered lines the minimum/ maximum values of the 5 recorded spectra.

(c) and (d): Lifetime of Flipper-TR in GUVs of different compositions DOPC (c) and 1:4 DOPC:Cholesterol (d) at different laser repetition rates and under two-photon excitation. Every dot represents fitted lifetime for 1 GUV, error bars are standard deviation and line is mean.

(e) Fluorescence lifetime images of GUVs from (c,d) under typical excitation conditions (20 MHz, 488 nm, top panel) and under two-photon excitation (80 MHz, 900 nm, bottom panel). Longer lifetime component is shown (shorter lifetime component fixed). Image size is 36.4*36.4 μm^2

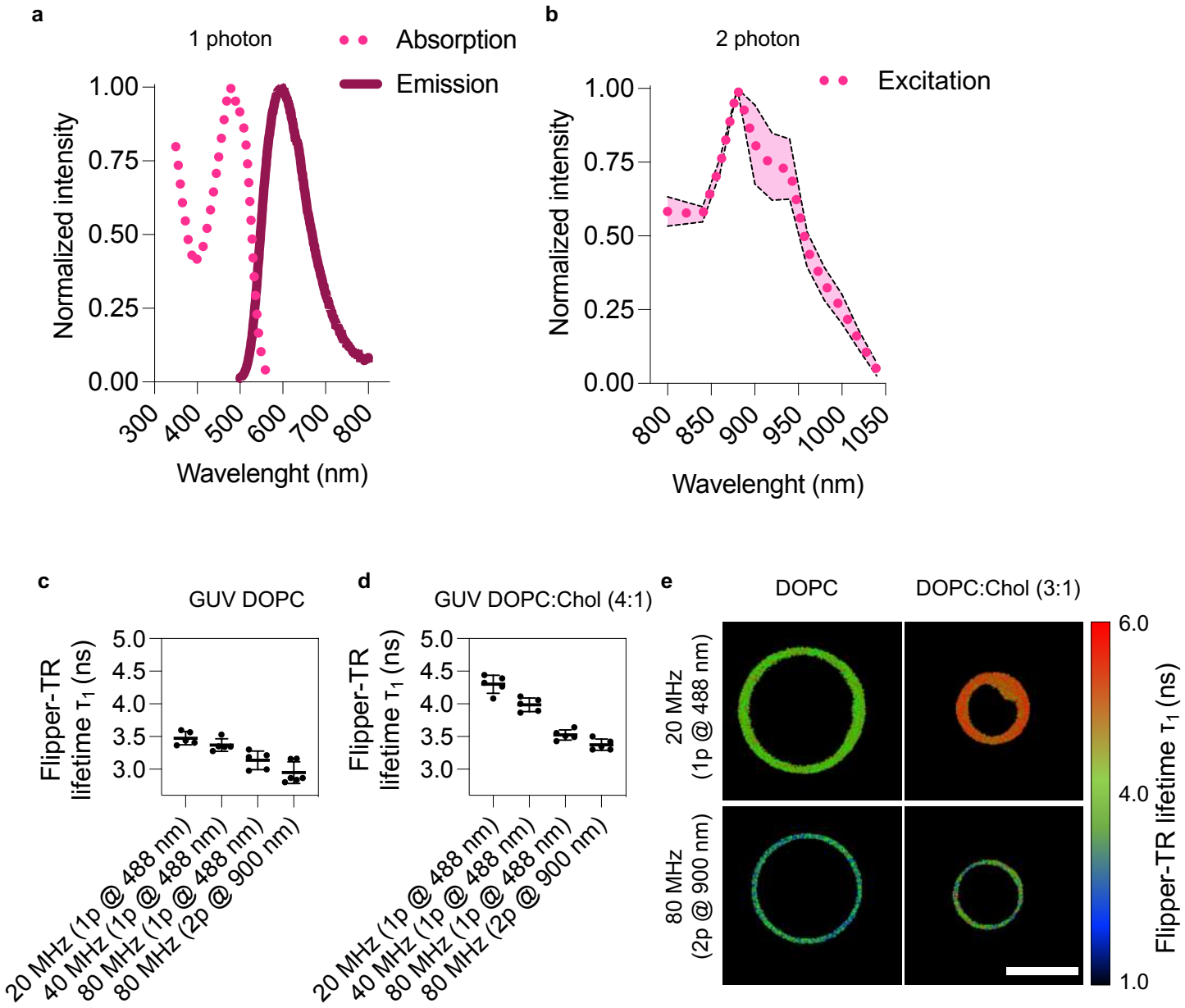
a
1 photon
Absorption
Emission
Normalized intensity
1.00
0.75
0.50
0.25
0.00
300
400
500
600
700
800
Wavelenght (nm)
b
2 photon
Excitation
Normalized intensity
1.00
0.75
0.50
0.25
0.00
800
850
900
950
1000
1050
Wavelenght (nm)
c
GUV DOPC
Flipper-TR lifetime τ1 (ns)
5.0
4.5
4.0
3.5
3.0
20 MHz (1p @ 488 nm)
40 MHz (1p @ 488 nm)
80 MHz (1p @ 488 nm)
80 MHz (2p @ 900 nm)
d
GUV DOPC:Chol (4:1)
Flipper-TR lifetime τ1 (ns)
5.0
4.5
4.0
3.5
3.0
20 MHz (1p @ 488 nm)
40 MHz (1p @ 488 nm)
80 MHz (1p @ 488 nm)
80 MHz (2p @ 900 nm)
e
DOPC
DOPC:Chol (3:1)
20 MHz (1p @ 488 nm)
80 MHz (2p @ 900 nm)
6.0
4.0
1.0
Flipper-TR lifetime τ1 (ns)

Extended Data Figure 2: Effect of linearly polarised excitation light on Flipper-TR lifetime measurements in GPMVs and GUVs.

(a) Intensity and (b) Lifetime images of cell-derived vesicles. Photoselection of the fixed excitation dipole of the Flipper-TR probe (using a linearly polarized excitation laser) causes bright rings with higher intensity. Graphs show (c) Lifetime and (d) intensity analysis of bright vs dark regions. Every dot represents the lifetime fit across one vesicle. The line represents the mean and error bars are standard deviation.

(e) Intensity and (f) lifetime and image of artificial vesicle composed of DOPC and Cholesterol (4:1). Image size is 36.4*36.4 μm^2. The graphs represent (g) lifetime and (h) intensity analysis of bright vs dark regions. Every dot represents the lifetime fit across one vesicle. The line represents the mean and error bars are standard deviation.

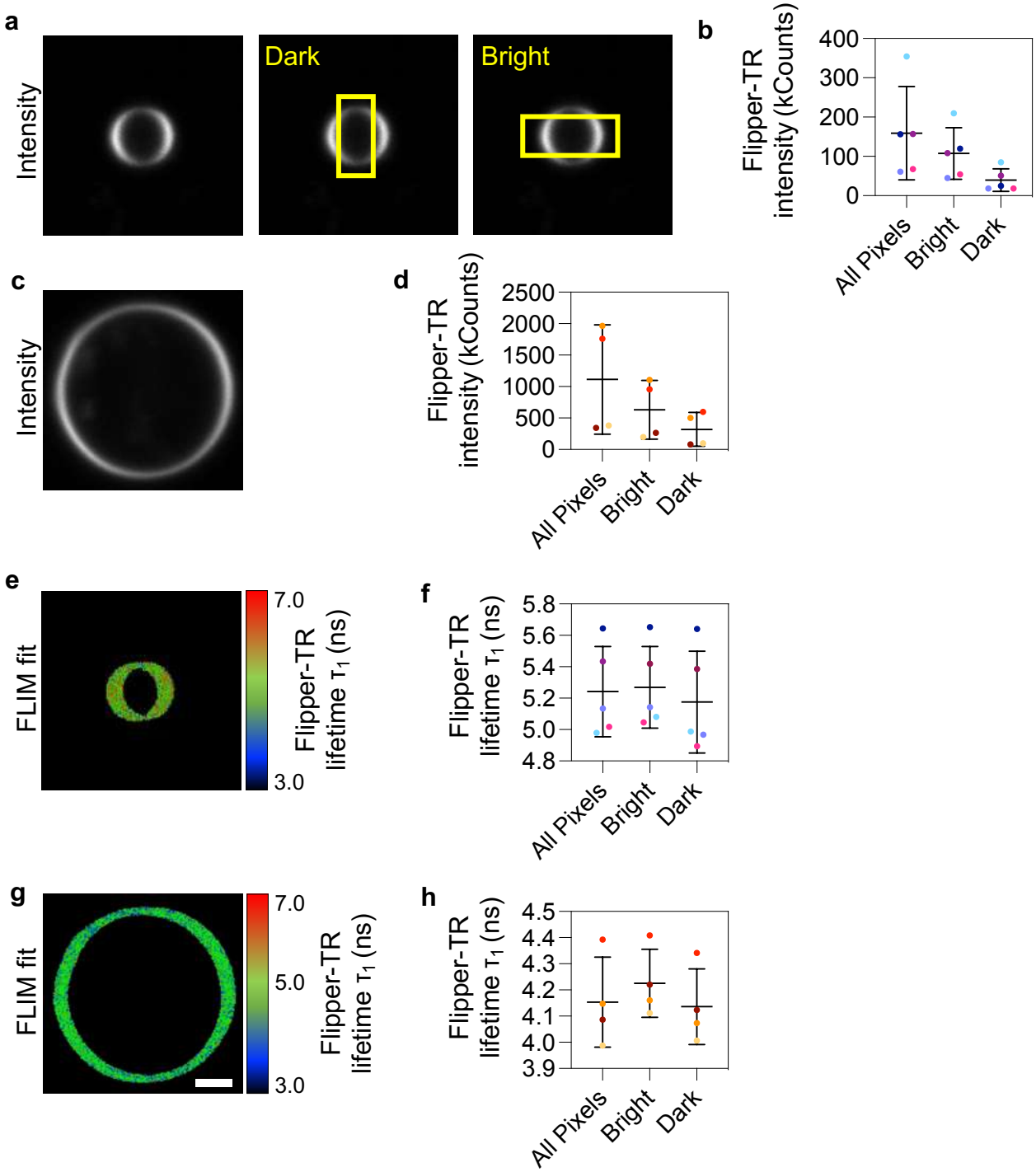
a
Intensity
Dark
Bright
b
Flipper-TR intensity (kCounts)
400
300
200
100
0
All Pixels
Bright
Dark
c
Intensity
d
Flipper-TR intensity (kCounts)
2500
2000
1500
1000
500
0
All Pixels
Bright
Dark
e
FLIM fit
7.0
3.0
Flipper-TR lifetime τ1 (ns)
f
Flipper-TR lifetime τ1 (ns)
5.8
5.6
5.4
5.2
5.0
4.8
All Pixels
Bright
Dark
g
FLIM fit
7.0
5.0
3.0
Flipper-TR lifetime τ1 (ns)
h
Flipper-TR lifetime τ1 (ns)
4.5
4.4
4.3
4.2
4.1
4.0
3.9
All Pixels
Bright
Dark